

## RESEARCH ARTICLE SUMMARY

## TOPOLOGICAL PHOTONICS

# Topological insulator laser: Theory

Gal Harari,\* Miguel A. Bandres,\* Yaakov Lumer, Mikael C. Rechtsman, Y. D. Chong, Mercedeh Khajavikhan, Demetrios N. Christodoulides, Mordechai Segev†

**INTRODUCTION:** Topological insulators emerged in condensed matter physics and constitute a new phase of matter, with insulating bulk and robust edge conductance that is immune to imperfections and disorder. To date, topological protection is known to be a ubiquitous phenomenon, occurring in many physical settings, ranging from photonics and cold atoms to acoustic, mechanical, and elastic systems. So far, however, most of these studies were carried out in entirely passive, linear, and conservative settings.

**RATIONALE:** We propose topological insulator lasers: lasers whose lasing mode exhibits topologically protected transport without magnetic fields. Extending topological physics to lasers is far from natural. In fact, lasers are built on foundations that are seemingly inconsistent with the essence of topological insulators: They require gain (and thus are

non-Hermitian), they are nonlinear entities because the gain must be saturable, and they are open systems because they emit light. These properties, common to all lasers, cast major doubts on the possibility of harnessing topological features to make a topological insulator laser. Despite this common mindset, we show that the use of topological properties leads to highly efficient lasers, robust to defects and disorder, with single-mode lasing even at conditions high above the laser threshold.

**RESULTS:** We demonstrate that topological insulator lasers are theoretically possible and experimentally feasible. We consider two configurations involving planar arrays of coupled active resonators. The first is based on the Haldane model, archetypical for topological systems. The second model, geared toward experiment, constitutes an aperiodic array architecture creating an artificial magnetic

field. We show that by introducing saturable gain and loss, it is possible to make these systems lase in a topological edge state. In this way, the lasing mode exhibits topologically protected transport; the light propagates unidirectionally along the edges of the cavity, immune to scattering and disorder,

## ON OUR WEBSITE

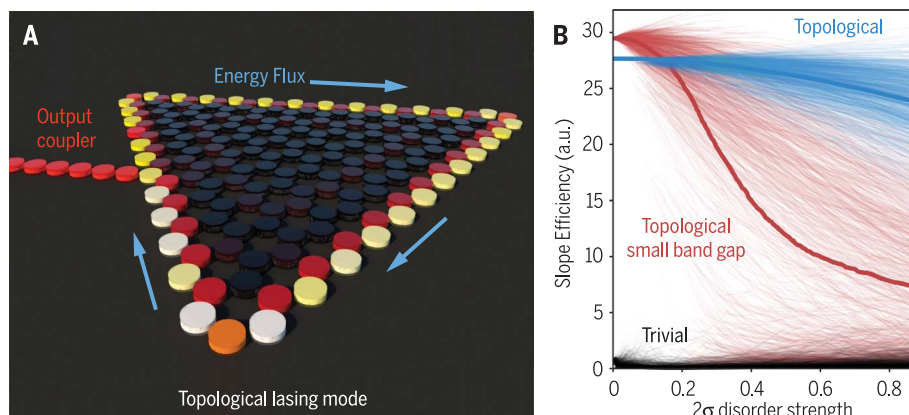
Read the full article at <http://dx.doi.org/10.1126/science.aar4003>

unaffected by the shape of the edges. Moreover, we show that the underlying topological properties not only make the system robust to fabrication and operational dis-

order and defects, they also lead to a highly efficient single-mode lasing that remains single-mode even at gain values high above the laser threshold.

The figure describes the geometry and features of a topological insulator laser based on the Haldane model while adding saturable gain, loss, and an output port. The cavity is a planar honeycomb lattice of coupled microring resonators, pumped at the perimeter with a lossy interior. We show that under these conditions, lasing occurs at the topological edge mode, which has unidirectional flux and is extended around the perimeter with almost-uniform intensity. The topological cavities exhibit higher efficiency than the trivial cavity, even under strong disorder. For the topological laser with a small gap, the topological protection holds as long as the disorder level is smaller than the gap size.

**DISCUSSION:** The concept of the topological insulator laser alters current understanding of the interplay between disorder and lasing, and opens exciting possibilities at the interface of topological physics and laser science, such as topologically protected transport in systems with gain. We show here that the laser system based on the archetypal Haldane model exhibits topologically protected transport, with features similar to those of its passive counterpart. This behavior means that this system is likely to have topological invariants, despite the non-hermiticity. Technologically, the topological insulator laser offers an avenue to make many semiconductor lasers operate as one single-mode high-power laser. The topological insulator laser constructed from an aperiodic array of resonators was realized experimentally in an all-dielectric platform, as described in the accompanying experimental paper by Bandres *et al.* ■



## Topological insulator laser based on the Haldane model and its efficiency.

(A) Planar honeycomb lattice of coupled microring resonators pumped at the perimeter. The topological lasing mode has unidirectional flux with almost-uniform intensity, which builds up as the mode circulates and drops when passing the output coupler. (B) Slope efficiency (in arbitrary units) versus disorder strength for three cases differing only in the Haldane phase (of the next-to-nearest neighbor coupling): a topological laser with the maximum gap (blue; Haldane phase of  $\pi/2$ ), one with a small topological gap (red; Haldane phase of  $\pi/8$ ), and a topologically trivial laser with no gap (black; Haldane phase of 0).

The list of author affiliations is available in the full article online.

\*These authors contributed equally to this work.

†Corresponding author. Email: [msegev@tx.technion.ac.il](mailto:msegev@tx.technion.ac.il)  
Cite this article as G. Harari *et al.*, *Science* 359, eaar4003 (2018). DOI: 10.1126/science.aar4003

## RESEARCH ARTICLE

## TOPOLOGICAL PHOTONICS

# Topological insulator laser: Theory

Gal Harari,<sup>1\*</sup> Miguel A. Bandres,<sup>1\*</sup> Yaakov Lumer,<sup>2</sup> Mikael C. Rechtsman,<sup>3</sup> Y. D. Chong,<sup>4</sup> Mercedeh Khajavikhan,<sup>5</sup> Demetrios N. Christodoulides,<sup>5</sup> Mordechai Segev<sup>1†</sup>

Topological insulators are phases of matter characterized by topological edge states that propagate in a unidirectional manner that is robust to imperfections and disorder. These attributes make topological insulator systems ideal candidates for enabling applications in quantum computation and spintronics. We propose a concept that exploits topological effects in a unique way: the topological insulator laser. These are lasers whose lasing mode exhibits topologically protected transport without magnetic fields. The underlying topological properties lead to a highly efficient laser, robust to defects and disorder, with single-mode lasing even at very high gain values. The topological insulator laser alters current understanding of the interplay between disorder and lasing, and at the same time opens exciting possibilities in topological physics, such as topologically protected transport in systems with gain. On the technological side, the topological insulator laser provides a route to arrays of semiconductor lasers that operate as one single-mode high-power laser coupled efficiently into an output port.

Topological insulators emerged in condensed matter physics (1–3) and constitute a new phase of matter, with insulating bulk and quantized and robust edge conductance. The prospect of observing topological effects in non-electronic systems was first proposed and demonstrated in microwaves in gyro-optic crystals with broken time-reversal symmetry (4–6). The transition to optical frequencies required another conceptual leap. Theoretical proposals (7–10) were followed by the first experiments using artificial gauge fields—one based on a honeycomb lattice of helical waveguides (11) and the other based on an array of aperiodic coupled silicon microring resonators (12). Topological protection is now known to be a ubiquitous phenomenon, occurring in physical settings as varied as electro-

magnetic waves (6, 11–16), cold atoms (17, 18), and acoustic, mechanical, and elastic systems (19–22). So far, however, most of these experiments have been carried out in entirely passive, linear, and conservative settings.

## Nonhermiticity in topological systems

Lasers represent complex nonconservative systems capable of exhibiting very rich dynamics. They are fundamentally non-Hermitian and nonlinear entities that rely on saturable gain. Introducing nonhermiticity to topological systems raises fundamental questions concerning whether non-Hermitian topological systems can exist at all (23), and if they do, how to define the topological phases and their stability (24). Part of this controversy has recently been resolved, and it is

now known that one-dimensional non-Hermitian systems can have stationary zero-dimensional topological edge states (25, 26) and topological defect states (27–29), and these can even lase (29–32). However, being one-dimensional systems lasing from a localized defect, none of these systems can support transport via edge states. Very recently, lasing from a topological edge state in a photonic crystal subject to an external magnetic field—a photonic analog of the quantum Hall effect—was reported (33). That system used magneto-optic effects, which are very weak at optical frequencies, and accordingly produced only a narrow topological band gap (40 pm) within which it was claimed that lasing occurred (33). Clearly, it will be important to pursue new approaches in expanding the topological photonic band gap, and hence the degree of protection endowed to such structures. Equally important, in terms of applications, will be to follow an all-dielectric strategy that is by nature compatible with semiconductor laser technologies.

Notwithstanding recent progress in topological photonics and lasing therein, the fundamental question is still open: Can topological protection of transport be incorporated into non-Hermitian, highly nonlinear, open systems such as lasers? Addressing this issue is at the heart of the topological insulator laser, along with many new questions: Can a topological insulator include gain, which has no equivalent in condensed matter physics? What happens to the stimulated emission under topologically protected transport? Can a topological insulator laser exist without a magnetic field, and if so, might it exhibit new features and improved laser action?

Laser cavities are typically optimized to attain high Q factors, and they are always strongly affected by disorder, which can arise from manufacturing imperfections, operational failure, stresses, etc. A prominent consequence of disorder is mode localization, which has dire implications in photonics (34, 35). To a laser, disorder implies degraded overlap of the lasing mode with the gain profile, lower output coupling, and multimode lasing, which together result in an overall reduced

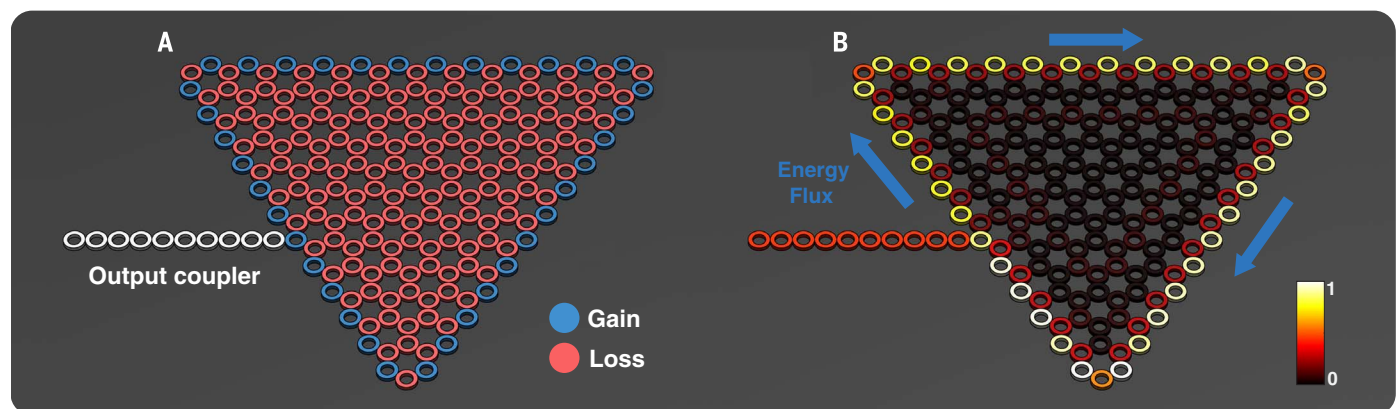


**Fig. 1. Geometry and lasing mode in a topological insulator laser based on the Haldane model.** (A) Cavity geometry (same for topological and trivial): a planar honeycomb lattice of coupled microring resonators. The cavity has unpumped (lossy) resonators (red), pumped resonators (blue), and an output channel (white). (B) The steady-state topological lasing mode

of the topological cavity. The lasing mode is extended all around the perimeter of the cavity with almost uniform intensity, and its energy flux is unidirectional. The unidirectional energy flux can be detected by the intensity buildup as the mode circulates (clockwise) and by the sudden drop in intensity when passing (clockwise) the output coupler.

efficiency. These problems are further exacerbated in more involved arrangements such as laser arrays. Such laser array structures tend to lase with many modes simultaneously, with their modal structure (near-field and spectrum) varying with the pumping strength. Despite many methods suggested to control the emission pattern of laser diode arrays, current technology is still not able to make the lasers operate as a single high-power coherent laser source. Consequently, the most common application of laser arrays is their usage as pumps (instead of flashtubes) for solid-state lasers but not as coherent high-power laser sources.

### Topological insulator lasers

Topological insulator lasers are lasers whose lasing mode exhibits topologically protected transport, such that the light propagates along the edges of the cavity in a unidirectional fashion, immune to

scattering and disorder, unaffected by the shape of the edges. We show that the underlying topological properties lead to a highly efficient laser, robust to fabrication and to operational disorder and defects, that exhibits single-mode lasing even at gain values high above the laser threshold.

We consider two possible configurations involving planar arrays of coupled, active resonators. The first is based on the Haldane model (36), an archetypical model for time reversal-broken topological insulators. The second relies on an aperiodic array architecture that creates an artificial magnetic field, as was demonstrated experimentally in passive systems (silicon) (8, 12, 13, 37). This is an all-dielectric system that has been realized with current semiconductor laser technology, as described in (38).

### Design of the topological laser cavity

In the Haldane design (36), the resonators of the topological insulator laser are arranged in a honeycomb lattice (Fig. 1A). Each resonator is coupled to its nearest neighbors by a real hopping parameter  $t_1$ , and to its next-nearest neighbors by a complex parameter  $t_2 \exp(i\phi)$ , where  $\phi$  is the Haldane flux parameter (39). The two sublattices of the honeycomb structure have identical on-site potentials. The passive Haldane model (no gain or loss, but  $t_2 \neq 0$ ) exhibits two phases: the trivial

phase when  $\phi$  is equal to 0 or  $\pi$ , and the topological phase when  $\phi \neq 0, \pi$ . In the topological phase, edge states emerge with energies extending across the topological gap that is proportional to  $t_2 \sin \phi$ , reaching a maximum at  $\phi = \pi/2$ . To promote the lasing of the topological edge mode, we specifically design the honeycomb array to have zig-zag edges that have small penetration depth into the bulk. The evolution of the field of this laser system is governed by

$$i \frac{\partial \Psi}{\partial t} = H_{\text{Haldane}} \Psi - i\gamma \Psi + \frac{ig\mathbb{P}}{1 + |\Psi|^2/I_{\text{sat}}} \Psi + H_{\text{output}} \Psi \quad (1)$$

where  $\Psi$  is a column vector encompassing the modal amplitudes of the array elements, and  $H_{\text{Haldane}}$  is the standard Haldane Hamiltonian (39), which depends on the resonance frequency of a single resonator  $\omega_0$ , the hopping constants  $t_{1,2}$ , and the Haldane flux  $\phi$ . Here,  $\gamma$  represents the loss in each resonator; this is assumed to be linear loss [as in all constant-wave lasers], although we simulated saturable loss as well, and our results were effectively the same. The third term in Eq. 1 represents optical gain via stimulated emission that is inherently saturable ( $I_{\text{sat}}$ ). Here,  $\mathbb{P}$  stands for the spatial profile of the pump, and  $H_{\text{output}}$  describes the output coupler

<sup>1</sup>Physics Department and Solid State Institute, Technion-Israel Institute of Technology, Haifa 32000, Israel.

<sup>2</sup>Department of Electrical and Systems Engineering, University of Pennsylvania, Philadelphia, PA 19104, USA.

<sup>3</sup>Department of Physics, Pennsylvania State University, University Park, PA 16802, USA. <sup>4</sup>Division of Physics and Applied Physics, Nanyang Technological University, 637371 Singapore. <sup>5</sup>CREOL, College of Optics and Photonics, University of Central Florida, Orlando, FL 32816, USA.

\*These authors contributed equally to this work.

†Corresponding author. Email: msegev@tx.technion.ac.il

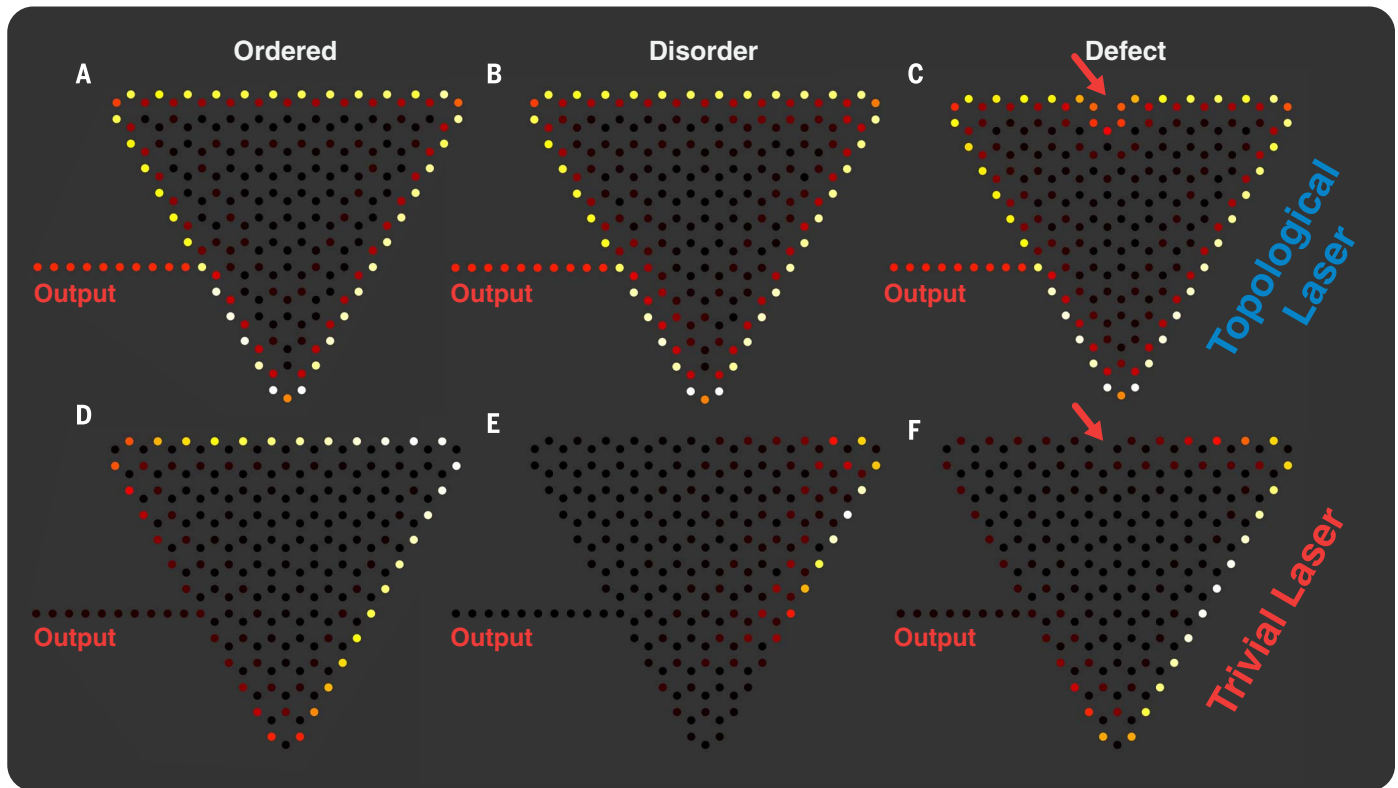
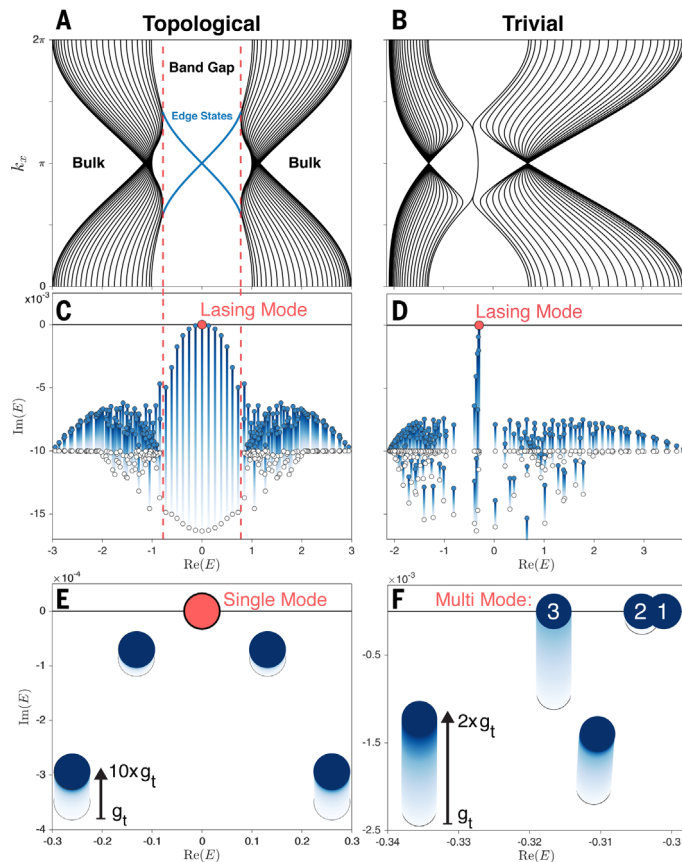


**Fig. 2. Lasing modes in the topological and trivial cavities (Haldane model).** (A to F) Steady-state lasing modes (colors indicate amplitude) for the topological and trivial cavities with no disorder [(A) and (D)], disorder [(B) and (E)], and a defect (a missing gain resonator at the perimeter) [(C) and (F)]. Being unidirectional and extended, with almost uniform intensity, the lasing mode in the topological cavity [(A) to (C)]

exhausts all the pumped sites and couples strongly to the output coupler in all cases. The trivial cavity, lacking unidirectional extended lasing modes, couples only weakly to the output coupler even without disorder (D). The presence of disorder (E) or defects (F) causes the lasing mode of the trivial cavity to be highly localized, further reducing the efficiency and the coupling to the output port.



**Fig. 3. The lasing process in the topological and trivial laser cavities. (A and B)** Band diagram of the passive (no gain or loss) topological (A) and trivial (B) strip of resonators. The topological cavity has a band gap with topologically protected unidirectional edge states crossing the gap (blue lines). By contrast, the trivial cavity has no protected transport, as there is no gap and the edge states are degenerate. **(C and D)** The evolution of the real and imaginary parts of the spectrum of the topological (C) and trivial (D) cavities, from zero gain (white dots) up to the threshold gain (blue dots), which is where the first lasing mode lases. **(E and F)** Evolution of the spectrum of the laser cavity modes as the gain is increased further above the threshold gain ( $g_t$ ). The topological laser (E) maintains single-mode lasing, at least up to gain values of 10 times the threshold gain. By contrast, the trivial laser (F) becomes multimode, with three lasing modes, at a gain level just twice the threshold gain.



(a semi-infinite chain of resonators, which is what makes this an open system) and its coupling to the cavity. To promote lasing of the edge modes, the gain ( $g$ ) is provided only to the resonators on the perimeter (Fig. 1A). In general,  $g$  is a function of the frequency; however, in semiconductors the gain is broadband (relative to the inter-ring coupling constant), and hence it is assumed to be frequency-independent.

### Topological insulator laser based on the Haldane model

We study the topological insulator laser by simulating the full dynamics and by directly solving for the nonlinear lasing modes of Eq. 1 (39). We consider two cases: (i) a trivial arrangement where  $\phi = 0$ , and (ii) a topological array when the Haldane flux is  $\phi = \pi/2$ . In the trivial case ( $\phi = 0$ ), even without disorder, the first lasing mode is localized away from the output coupler (Fig. 2D) so as to minimize the power loss through the coupler. This strongly affects the lasing efficiency because the localized lasing mode does not use all the gain available around the perimeter and it is coupled only very weakly to the output. This adversarial effect is further enhanced in the presence of disorder, given that it tends to highly localize modes. For example (Fig. 2E), in the presence of disorder, the lasing mode of the trivial

cavity becomes further confined within just a few resonators. Finally, because the trivial lasing mode does not spatially deplete the gain, if pumped harder, multiple modes can reach threshold, giving rise to multimode operation (Fig. 3F).

In the topological case ( $\phi = \pi/2$ ), the lasing mode possesses all the distinct characteristics of topological chiral edge states: It is extended all around the perimeter of the cavity with almost-uniform intensity, and its energy flux is unidirectional. The unidirectionality of the energy flux can be observed by noticing how the energy starts accumulating while moving clockwise around the perimeter of the array, and then abruptly drops after the output coupler (Fig. 1B). Even though the notion of topological invariants in non-Hermitian, nonlinear open systems (such as lasers) is still largely unexplored, the topological nature of this array can be recognized by observing its dynamics. In this regard, it is instructive to monitor the evolution in the system, from below transparency to lasing. Figure 3, C and D, shows the behavior of the complex frequency of the cavity modes as we increase the gain from zero to the threshold level. During this process, the frequency (real part) of each mode is virtually unchanged, equal to the eigenfrequencies of the closed Hermitian system (the topological insulator lattice), and the band gap of

the topological system (blue region in Fig. 3A) remains well defined and constant. Clearly, the topological band gap does not close in the presence of gain (even high above the threshold level), and no topological phase transition occurs. This is a clear indication that the system retains its topological features even when it lases. More important, as shown in Fig. 3C, one of the topological edge modes is the first in line to lase. Moreover, even when we increase the gain (pumping) high above the threshold level, the lasing remains in a single mode—the topological edge mode. This is because the topological lasing mode has almost uniform intensity all around the perimeter of the array, saturating the whole gain medium, hence suppressing all the other cavity modes and preventing them from lasing (Fig. 3E).

To further examine the topological properties of the lasing mode, we study the system in the presence of disorder and defects. We find that even in the presence of disorder, the topological insulator laser still operates in a topological edge mode (Fig. 2B). Even when a defect is introduced—for example, a malfunctioning microring at the perimeter—the topological edge mode is able to bypass the defect with minimal penetration into the bulk (Fig. 2C).

It is instructive to highlight the role of topology in this topological insulator laser by comparing its efficiency to its trivial counterpart. The efficiency of lasers is universally defined by the so-called “slope efficiency”: the slope of the function describing the output power as a function of gain above the threshold level. The calculated slope efficiencies (in steady state) as a function of the strength of the disorder are shown in Fig. 4A. When the cavity is in the trivial phase,  $\phi = 0$ , the slope efficiency is poor and further decreases in the presence of disorder. In sharp contrast, when the laser is topological,  $\phi = \pi/2$ , the lasing is very efficient and robust; it has a high slope efficiency (with a small variance) that remains high even at strong disorder levels. The topological protection ceases only when the strength of disorder is comparable to the size of the topological band gap. To reaffirm that the high efficiency of this laser is due to its topological protection, we evaluate the slope efficiency for structures with a smaller band gap (e.g., for  $\phi = \pi/8$ ). As seen in Fig. 4A, the slope efficiency of this “small topological gap implementation” is initially high, but when the level of disorder is increased, it deteriorates much faster than the  $\phi = \pi/2$  case, because the disorder closes the smaller topological gap more easily. To further highlight the robustness of our topological insulator laser, we calculate the mean value of the slope efficiency as a function of disorder strength and the two main parameters that control the size of the topological band gap: the Haldane flux (Fig. 4B) and the next-nearest neighbor coupling  $t_2$  (Fig. 4C). When the strength of randomness is less than the size of the Haldane topological band gap ( $6\sqrt{3}t_2 \sin \phi$ ), the slope efficiency stays high, and drops only when the disorder level exceeds the size of the topological band gap (Fig. 4, B and C). This is a clear indication that the efficiency and robustness of the

topological insulator laser arise from its topological properties (40).

### Topological insulator laser based on an aperiodic array of resonators

Next, we study lasing in an aperiodic topological array of microring resonators, which was one of the two platforms first explored for realizing photonic topological insulators in optics (8, 12). This arrangement involves a lattice of coupled resonators with aperiodic couplers (39)—an architecture that can be implemented using standard semiconductor technologies (41, 42). Note that this system does not use magnetic fields, nor does it use any exotic materials (such as yttrium iron garnet). It relies only on present semiconductor laser technology. The aperiodic couplers establish an artificial gauge field, thus leading to behavior analogous to the quantum Hall effect (12). Because in the linear regime the system is reciprocal, both the clockwise (CW) and counterclockwise (CCW) modes in each microring resonator experience gauge fields with opposite signs. This, in turn, makes the overall cavity degenerate; that is, for any frequency supported by the CW modes, there is a corresponding CCW mode. In passive settings (no gain or loss), for reasonable experimental parameters, one can consider the CW and CCW as decoupled (8, 12). For a topological insulator laser based on this system, one must take into account that the CW and CCW modes inevitably interact with one another through the nonlinear effect of gain saturation and backscattering, both of which naturally occur in active media (43).

This topological aperiodic laser array is simulated using an extended version of Eq. 1 (39). To account for a realistic setup in current semiconductor laser technology, we implement saturable

gain and explicit coupling between the CW and CCW modes through the saturable medium and backscattering. We use the parameters of recent experiments (42) and of the accompanying experimental paper (38), which yield a topological band gap of  $\sim 1$  nm, in an aperiodic ring array made of all-dielectric semiconductor laser materials. A topological gap of this size ensures very high topological protection of transport in the laser cavity. We essentially observe the same features as in the Haldane model: The topological lasing mode is extended, uniform, and couples strongly to the output coupler, even in the presence of disorder. In contrast, the topologically trivial aperiodic array, having no edge modes, suffers from localization of its lasing modes and displays strong multimode lasing and low output coupling (Fig. 5). It is important to stress that despite the reciprocity of the system and the inherent degeneracy of every ring and the presence of scattering and saturable gain (which cause lasing in both the CW and CCW directions), the topologically protected features of the lasing modes prevail, and the efficiency of the topological array is much higher than that of the trivial case. The underlying mechanism can be clearly seen from the mode shapes in Fig. 5, B to E, where the mutual contribution of the two counterpropagating (CW and CCW) edge modes with the same temporal frequency depletes the gain and enforces efficient single-frequency lasing. In a similar vein, the topological lasing modes exhibit high robustness against defects and disorder, despite the backscattering and the nonlinear coupling between the CW and CCW modes.

### Concluding remarks

As a result of its topological properties, the topological insulator laser exhibits high efficiency,

extreme robustness to defects and disorder, and high-efficiency single-mode lasing even at gain levels high above the threshold level. The interplay between topology and nonhermiticity, especially in nonlinear open systems such as lasers, raises many fundamental questions. We have shown that the laser system based on the archetypal Haldane model exhibits topologically protected transport, with features similar to its passive counterpart. This behavior means that there must be associated topological invariants, even though this system is non-Hermitian. Topologically protected transport in lasing systems can change existing paradigms by harnessing the topological features of the lasing mode to yield high-efficiency single-mode lasing even high above threshold.

The systems proposed here are a proof of concept, with no attempt to optimize the integration of topological properties into a laser. The topological design of the laser cavity can take on many different concrete designs, which may lead to new ideas and innovative applications. For example, the topological system can be based on topological network models of strongly coupled resonators (44), which can be realized with very small units. More generally, new geometries, wherein a medium with narrow-linewidth gain is matched to the topological gap, can be considered. In a similar vein, topological insulator lasers could be designed from flexible gain media (organics), and operate under distortions, manipulations, and perhaps also extreme conditions. It may even be possible to integrate topological insulator lasers with sensors, antennas, and other photonic devices. The accompanying paper (38) describes the realization of a topological insulator laser without magnetic field. It is an all-dielectric system, based on the aperiodic array of ring resonators described here, fabricated with

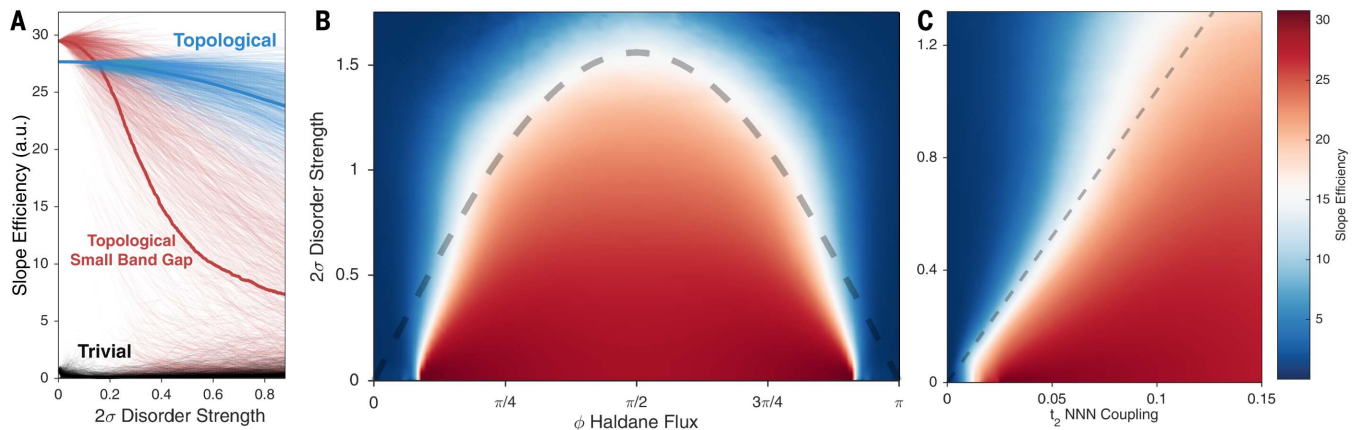


**Fig. 4. Slope efficiency versus disorder in the topological and trivial laser systems (Haldane model).** (A) Slope efficiency (in arbitrary units) versus disorder strength (measured in terms of its standard deviation) for the topological laser with the maximum gap (blue;  $\phi = \pi/2$ ) and with a small topological gap (red;  $\phi = \pi/8$ ), and for the trivial laser with no gap (black;  $\phi = 0$ ). Every point corresponds to the slope efficiency of a different realization of the disorder (1000 in total). Solid lines mark the mean values for each case. The topological cavities exhibit higher slope efficiency (blue line) than the trivial cavity, even under high levels of disorder. For the topological insulator laser with

a small band gap, when the disorder level is increased to above the band gap size, the topological protection of this topological laser starts to break and its efficiency is markedly deteriorated (red line). (B and C) Mean value of slope efficiency (average over 1000 realizations) as a function of disorder and Haldane flux  $\phi$  (B) and as a function of disorder and next-nearest neighbor coupling  $t_2$  (C). The dashed black lines depict the size of the band gap of the Haldane model at zero disorder, given by  $6\sqrt{3}t_2 \sin \phi$ . Clearly, the slope efficiency of the topological cavity stays high as long as the disorder strength is lower than the size of the topological gap.



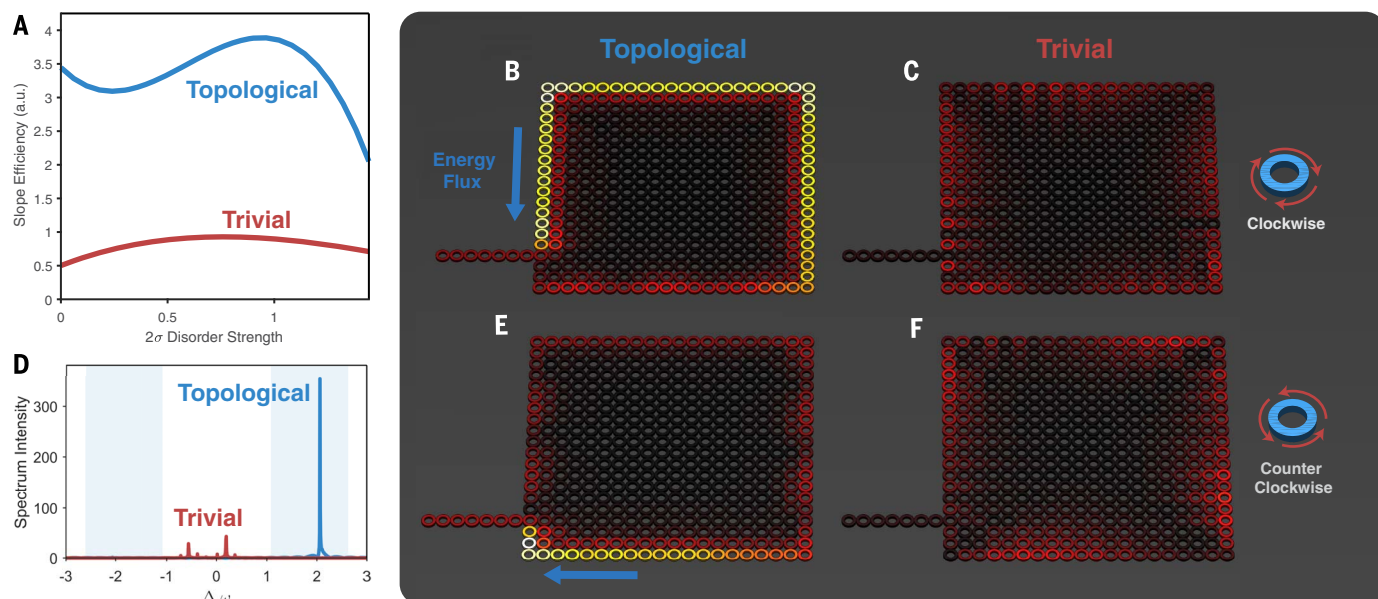


**Fig. 5. Lasing modes in the topological and trivial cavities (coupled-resonators model).** (A) Mean slope efficiency as a function of disorder strength (measured in terms of the standard deviation of the on-site energy) for the topological laser (blue) and the trivial laser (red). The simulation includes 5% backscattering on each site. The slope efficiency of the topological laser is higher and more robust up to disorder levels on the order of the topological band gap. (B, C, E, and F) Typical lasing modes (colors indicate amplitude as indicated in Fig. 1) for the topological [(B) and (E)] and the trivial [(C) and (F)] cavities. The first and second rows show the CW and CCW components, respectively. In the topological array, the CW (B) and

CCW (E) components travel in opposite directions around the lattice but they both lase at the same frequency, synergistically transporting energy from the pumped sites to the output coupler. By contrast, in the trivial lattice [(C) and (F)], the modes become localized in the presence of disorder, penetrate into the lossy bulk, and couple only weakly to the output coupler. (D) Spectra of the topological (blue) and the trivial (red) lasers for the same level of pumping. Even in the presence of disorder and backscattering, the topological array lases in a single mode inside one of the topological band gaps (shaded blue regions), whereas the trivial array, for the same gain and disorder levels, lases weakly and at multiple frequencies.

ordinary technology for making semiconductor lasers.

## REFERENCES AND NOTES

- C. L. Kane, E. J. Mele, Quantum spin Hall effect in graphene. *Phys. Rev. Lett.* **95**, 226801 (2005). PMID: 16384250
- B. A. Bernevig, T. L. Hughes, S.-C. Zhang, Quantum spin Hall effect and topological phase transition in HgTe quantum wells. *Science* **314**, 1757–1761 (2006). doi: [10.1126/science.1133734](https://doi.org/10.1126/science.1133734); PMID: 17170299
- M. König et al., Quantum spin Hall insulator state in HgTe quantum wells. *Science* **318**, 766–770 (2007). doi: [10.1126/science.1148047](https://doi.org/10.1126/science.1148047); PMID: 17885096
- S. Raghu, F. Haldane, Analogs of quantum-Hall-effect edge states in photonic crystals. *Phys. Rev. A* **78**, 033834 (2008). doi: [10.1103/PhysRevA.78.033834](https://doi.org/10.1103/PhysRevA.78.033834)
- Z. Wang, Y. D. Chong, J. D. Joannopoulos, M. Soljacic, Reflection-free one-way edge modes in a gyromagnetic photonic crystal. *Phys. Rev. Lett.* **100**, 013905 (2008). doi: [10.1103/PhysRevLett.100.013905](https://doi.org/10.1103/PhysRevLett.100.013905); PMID: 18232767
- Z. Wang, Y. Chong, J. D. Joannopoulos, M. Soljacic, Observation of unidirectional backscattering-immune topological electromagnetic states. *Nature* **461**, 772–775 (2009). doi: [10.1038/nature08293](https://doi.org/10.1038/nature08293); PMID: 19812669
- R. O. Umucalilar, I. Carusotto, Artificial gauge field for photons in coupled cavity arrays. *Phys. Rev. A* **84**, 043804 (2011). doi: [10.1103/PhysRevA.84.043804](https://doi.org/10.1103/PhysRevA.84.043804)
- M. Hafezi, E. Demler, M. Lukin, J. Taylor, Robust optical delay lines via topological protection. *Nat. Phys.* **7**, 907–912 (2011). doi: [10.1038/nphys2063](https://doi.org/10.1038/nphys2063)
- K. Fang, Z. Yu, S. Fan, Realizing effective magnetic field for photons by controlling the phase of dynamic modulation. *Nat. Photonics* **6**, 782–787 (2012). doi: [10.1038/nphoton.2012.236](https://doi.org/10.1038/nphoton.2012.236)
- A. B. Khanikaev et al., Photonic topological insulators. *Nat. Mater.* **12**, 233–239 (2013). PMID: 23241532
- M. C. Rechtsman et al., Photonic Floquet topological insulators. *Nature* **496**, 196–200 (2013). doi: [10.1038/nature12066](https://doi.org/10.1038/nature12066); PMID: 23579677
- M. Hafezi, S. Mittal, J. Fan, A. Migdall, J. M. Taylor, Imaging topological edge states in silicon photonics. *Nat. Photonics* **7**, 1001–1005 (2013). doi: [10.1038/nphoton.2013.274](https://doi.org/10.1038/nphoton.2013.274)
- S. Mittal et al., Topologically robust transport of photons in a synthetic gauge field. *Phys. Rev. Lett.* **113**, 087403 (2014). doi: [10.1103/PhysRevLett.113.087403](https://doi.org/10.1103/PhysRevLett.113.087403); PMID: 25192126
- X. Cheng et al., Robust reconfigurable electromagnetic pathways within a photonic topological insulator. *Nat. Mater.* **15**, 542–548 (2016). doi: [10.1038/nmat4573](https://doi.org/10.1038/nmat4573); PMID: 26901513
- V. Peano, M. Houde, F. Marquardt, A. A. Clerk, Topological quantum fluctuations and traveling wave amplifiers. *Phys. Rev. X* **6**, 041026 (2016). doi: [10.1103/PhysRevX.6.041026](https://doi.org/10.1103/PhysRevX.6.041026)
- A. P. Slobozhanyuk et al., Experimental demonstration of topological effects in bianisotropic metamaterials. *Sci. Rep.* **6**, 22270 (2016). doi: [10.1038/srep22270](https://doi.org/10.1038/srep22270); PMID: 26936219
- M. Aidelburger et al., Measuring the Chern number of Hofstadter bands with ultracold bosonic atoms. *Nat. Phys.* **11**, 162–166 (2015). doi: [10.1038/nphys3171](https://doi.org/10.1038/nphys3171)
- G. Jotzu et al., Experimental realization of the topological Haldane model with ultracold fermions. *Nature* **515**, 237–240 (2014). doi: [10.1038/nature13915](https://doi.org/10.1038/nature13915); PMID: 25391960
- L. M. Nash et al., Topological mechanics of gyroscopic metamaterials. *Proc. Natl. Acad. Sci. U.S.A.* **112**, 14495–14500 (2015). doi: [10.1073/pnas.1507431112](https://doi.org/10.1073/pnas.1507431112); PMID: 26561580
- Z. Yang et al., Topological acoustics. *Phys. Rev. Lett.* **114**, 114301 (2015). doi: [10.1103/PhysRevLett.114.114301](https://doi.org/10.1103/PhysRevLett.114.114301); PMID: 25839273
- P. Wang, L. Lu, K. Bertoldi, Topological phononic crystals with one-way elastic edge waves. *Phys. Rev. Lett.* **115**, 104302 (2015). doi: [10.1103/PhysRevLett.115.104302](https://doi.org/10.1103/PhysRevLett.115.104302); PMID: 26382680
- C. L. Kane, T. C. Lubensky, Topological boundary modes in isostatic lattices. *Nat. Phys.* **10**, 39–45 (2013). doi: [10.1038/nphys2835](https://doi.org/10.1038/nphys2835)
- Y. C. Hu, T. L. Hughes, Absence of topological insulator phases in non-Hermitian PT-symmetric Hamiltonians. *Phys. Rev. B* **84**, 153101 (2011). doi: [10.1103/PhysRevB.84.153101](https://doi.org/10.1103/PhysRevB.84.153101)
- K. Esaki, M. Sato, K. Hasebe, M. Kohmoto, Edge states and topological phases in non-Hermitian systems. *Phys. Rev. B* **84**, 205128 (2011). doi: [10.1103/PhysRevB.84.205128](https://doi.org/10.1103/PhysRevB.84.205128)
- M. S. Rudner, L. S. Levitov, Topological transition in a non-Hermitian quantum walk. *Phys. Rev. Lett.* **102**, 065703 (2009). doi: [10.1103/PhysRevLett.102.065703](https://doi.org/10.1103/PhysRevLett.102.065703); PMID: 19257606
- J. M. Zeuner et al., Observation of a topological transition in the bulk of a non-Hermitian system. *Phys. Rev. Lett.* **115**, 040402 (2015). doi: [10.1103/PhysRevLett.115.040402](https://doi.org/10.1103/PhysRevLett.115.040402); PMID: 26252670
- S. D. Liang, G. Y. Huang, Topological invariance and global Berry phase in non-Hermitian systems. *Phys. Rev. A* **87**, 012118 (2013). doi: [10.1103/PhysRevA.87.012118](https://doi.org/10.1103/PhysRevA.87.012118)
- S. Weimann et al., Topologically protected bound states in photonic parity-time-symmetric crystals. *Nat. Mater.* **16**, 433–438 (2017). PMID: 27918567
- H. Zhao, P. Miao, M. H. Teimourpour, S. Malzard, R. El-Ganainy, H. Schomerus, L. Feng, Topological hybrid silicon microlasers. *arXiv:1709.02747* (2017).
- L. Pilozi, C. Conti, Topological lasing in resonant photonic structures. *Phys. Rev. B* **93**, 195317 (2016). doi: [10.1103/PhysRevB.93.195317](https://doi.org/10.1103/PhysRevB.93.195317)
- P. St-Jean, V. Goblot, E. Galopin, A. Lemaître, T. Ozawa, L. Le Gratiet, I. Sagnes, J. Bloch, A. Amo, Lasing in topological edge states of a 1D lattice. *arXiv:1704.07310* (2017).
- M. Parto, S. Wittek, H. Hodaei, G. Harari, M. A. Bandres, J. Ren, M. C. Rechtsman, M. Segev, D. N. Christodoulides, M. Khajavikhan, Complex edge-state phase transitions in 1D topological laser arrays. *arXiv:1709.00523* (2017).
- B. Bahari et al., Nonreciprocal lasing in topological cavities of arbitrary geometries. *Science* **358**, 636–640 (2017). PMID: 29025992
- M. Segev, Y. Silberberg, D. Christodoulides, Anderson localization of light. *Nat. Photonics* **7**, 197–204 (2013). doi: [10.1038/nphoton.2013.30](https://doi.org/10.1038/nphoton.2013.30)
- J. Liu et al., Random nanolasing in the Anderson localized regime. *Nat. Nanotechnol.* **9**, 285–289 (2014). doi: [10.1038/nnano.2014.34](https://doi.org/10.1038/nnano.2014.34); PMID: 24658170
- F. D. M. Haldane, Model for a quantum Hall effect without Landau levels: Condensed-matter realization of the “parity anomaly”. *Phys. Rev. Lett.* **61**, 2015–2018 (1988). doi: [10.1103/PhysRevLett.61.2015](https://doi.org/10.1103/PhysRevLett.61.2015); PMID: 10038961

37. S. Mittal, S. Ganeshan, J. Fan, A. Vaezi, M. Hafezi, Measurement of topological invariants in a 2D photonic system. *Nat. Photonics* **10**, 180–183 (2016). doi: [10.1038/nphoton.2016.10](https://doi.org/10.1038/nphoton.2016.10)
38. M. A. Bandres *et al.*, Topological insulator laser: Experiment. *Science* **359**, eaar4005 (2018). doi: [10.1038/nphoton.2016.10](https://doi.org/10.1038/nphoton.2016.10)
39. See supplementary materials.
40. For completeness, we also studied the operation of the laser when the same system has a trivial gap, with no edge states crossing the gap. To open a trivial gap, we detuned the resonance frequencies of the resonators associated with the two sublattices of the Haldane model. When the detuning was large enough, it opened a topologically trivial band gap even with  $\phi = \pi/2$ , but this trivial gap does not yield topological protection nor high-efficiency lasing. We found that the efficiency of the laser is high and robust to disorder only when the gap is topological.
41. L. Feng, Z. J. Wong, R. M. Ma, Y. Wang, X. Zhang, Single-mode laser by parity-time symmetry breaking. *Science* **346**, 972–975 (2014). doi: [10.1126/science.1258479](https://doi.org/10.1126/science.1258479); pmid: [25414307](https://pubmed.ncbi.nlm.nih.gov/25414307/)
42. H. Hodaei, M. A. Miri, M. Heinrich, D. N. Christodoulides, M. Khajavikhan, Parity-time-symmetric microring lasers. *Science* **346**, 975–978 (2014). doi: [10.1126/science.1258480](https://doi.org/10.1126/science.1258480); pmid: [25414308](https://pubmed.ncbi.nlm.nih.gov/25414308/)
43. D. Liu *et al.*, Symmetry, stability, and computation of degenerate lasing modes. *Phys. Rev. A* **95**, 023835 (2016). doi: [10.1103/PhysRevA.95.023835](https://doi.org/10.1103/PhysRevA.95.023835)
44. G. Q. Liang, Y. D. Chong, Optical resonator analog of a two-dimensional topological insulator. *Phys. Rev. Lett.* **110**, 203904 (2013). doi: [10.1103/PhysRevLett.110.203904](https://doi.org/10.1103/PhysRevLett.110.203904); pmid: [25167412](https://pubmed.ncbi.nlm.nih.gov/25167412/)

#### ACKNOWLEDGMENTS

**Funding:** Supported by Singapore MOE Academic Research Fund Tier 2 Grant MOE2015T2-2-008 and Tier 3 Grant MOE2016-T3-1006 (C.Y.D.); Penn State NSF MRSEC Center for Nanoscale Science (under award NSF DMR-1420620), NSF grant DMS-1620422, and the Packard, Sloan, and Kaufman foundations (M.C.R.); the Israel Science Foundation; Office of Naval Research grant N0001416-1-2640; NSF grants ECCS 1454531, DMR-1420620, and ECCS 1757025; U.S. Air Force Office of Scientific Research grant FA9550-14-1-0037; U.S.-Israel Binational Science Foundation

grant 2016381; the German-Israeli Deutsch-Israelische Projektkooperation program; Army Research Office grants W911NF-16-1-0013 and W911NF-17-1-0481; and ERC grant NHQWAVE (MSCA-RISE 691209). M.S. thanks M. Karpovsky and B. Shillman for their support that came at a critical time. **Author contributions:** All authors contributed to all aspects of this work. **Competing interests:** The authors declare no competing financial interests. **Data and materials availability:** All data needed to evaluate the conclusions in the paper are present in the paper and/or the supplementary materials.

#### SUPPLEMENTARY MATERIALS

[www.sciencemag.org/content/359/6381/eaar4003/suppl/DC1](http://www.sciencemag.org/content/359/6381/eaar4003/suppl/DC1)  
Materials and Methods  
Figs. S1 and S2  
References (45, 46)

3 November 2017; accepted 17 January 2018  
Published online 1 February 2018  
[10.1126/science.aar4003](https://doi.org/10.1126/science.aar4003)

## Topological insulator laser: Theory

Gal Harari, Miguel A. Bandres, Yaakov Lumer, Mikael C. Rechtsman, Y. D. Chong, Mercedeh Khajavikhan, Demetrios N. Christodoulides and Mordechai Segev

*Science* **359** (6381), eaar4003.

DOI: 10.1126/science.aar4003originally published online February 1, 2018

### Topological protection for lasers

Ideas based on topology, initially developed in mathematics to describe the properties of geometric space under deformations, are now finding application in materials, electronics, and optics. The main driver is topological protection, a property that provides stability to a system even in the presence of defects. Harari *et al.* outline a theoretical proposal that carries such ideas over to geometrically designed laser cavities. The lasing mode is confined to the topological edge state of the cavity structure. Bandres *et al.* implemented those ideas to fabricate a topological insulator laser with an array of ring resonators. The results demonstrate a powerful platform for developing new laser systems.

*Science*, this issue p. eaar4003, p. eaar4005

#### ARTICLE TOOLS

<http://science.sciencemag.org/content/359/6381/eaar4003>

#### SUPPLEMENTARY MATERIALS

<http://science.sciencemag.org/content/suppl/2018/01/31/science.aar4003.DC1>

#### RELATED CONTENT

<http://science.sciencemag.org/content/sci/359/6381/eaar4005.full>

#### REFERENCES

This article cites 38 articles, 5 of which you can access for free  
<http://science.sciencemag.org/content/359/6381/eaar4003#BIBL>

#### PERMISSIONS

<http://www.sciencemag.org/help/reprints-and-permissions>

Use of this article is subject to the [Terms of Service](#)

---

*Science* (print ISSN 0036-8075; online ISSN 1095-9203) is published by the American Association for the Advancement of Science, 1200 New York Avenue NW, Washington, DC 20005. The title *Science* is a registered trademark of AAAS.

Copyright © 2018 The Authors, some rights reserved; exclusive licensee American Association for the Advancement of Science. No claim to original U.S. Government Works